Crustal structure of northern Borneo from VDSS: Implications for subduction termination and the tectonic reconstruction of SE Asia

H. T. Linang[1], S. Pilia[1,2], N. Rawlinson[1], C. A. Bacon[1], A. Gilligan[3], D. G. Cornwell[3], F. Tongkul[4]

[1] Bullard Laboratories, University of Cambridge, Cambridge, UK, [2] Department of Earth and Environmental Sciences, University of Milan-Bicocca, Milan, Italy, [3] Department of Geology and Geophysics, University of Aberdeen, Aberdeen, UK, [4] Faculty of Science and Natural Resource, Universiti of Malaysia Sabah, Kota Kinabalu, Sabah, Malaysia.

Corresponding author: Harry Telajan Linang (htal3@cam.ac.uk)

Key Points:

- Crustal thickness map of northern Borneo obtained from Virtual Deep Seismic Sounding (VDSS).
- Evidence of crustal thinning indicates Sulu Sea extension propagated into northern Borneo during the late Miocene.
- Crustal thinning and newly computed focal mechanism solutions underscore the important role of extension in post-collisional settings.

Abstract

The post-subduction tectonic evolution of northern Borneo, which experienced two sequential subduction episodes of opposite polarity in the Neogene, is still widely debated with first-order questions, such as whether the region has been in a state of compression or extension, remaining unresolved. We use waveform data recorded from a dense seismic network in northern Borneo to investigate crustal thickness variations through the application of Virtual Deep Seismic Sounding (VDSS). The new results reveal an extensive area of thin crust in central and southeastern Sabah that appears to extend northeast into the Sulu Sea, where rifting initiated. We also compute local earthquake focal mechanisms, which suggest that extension is ongoing, though now dominated by orogen collapse in the NW. Together these results point to the pervasiveness of regional extension over the last 15-20 Myr and its role in the post-subduction cycle of plate tectonics in SE Asia.

Plain Language Summary

Northern Borneo, which lies in the heart of southeast Asia, was assembled by a complex series of tectonic events over the last 40 million years. Principle among these was subduction of the Proto South China Sea plate beneath its northwest continental margin, which ended in continent-continent collision. Subduction of the Celebes Sea plate in the SW followed, which terminated ~ 9 million years ago. A key point of debate in the evolution of this region is the relative dominance of compressional and extensional tectonics. In this study, we exploit seismic data collected in northern Borneo from a dense array of seismometers to construct a new crustal model of the region, which robustly constrains the crust-mantle boundary. We find that the crust in central northern Borneo is anomalously thin and appears to extend NE into the Sulu Sea, which is consistent with a model of rifting and ocean basin formation that propagated into the adjacent continent. An

analysis of earthquake sources also indicate a predominance of normal faulting, which suggests that extensional tectonics likely dominated the region following the earlier continent-continent collision. This finding has important implications for understanding both post-collisional and post-subduction processes and the assembly of Southeast Asia.

Introduction

Northern Borneo, which incorporates the Malaysian state of Sabah, represents a unique opportunity to understand the evolution of continental lithosphere in a post-subduction setting, in this case, produced by sequential termination of two opposed subduction systems in the Miocene, and holds vital clues for unraveling the complex tectonic history of Southeast Asia (e.g., Rangin, 1990; Hutchison, 2000; Hall, 2008; Hall, 2013; Tongkul, 2017). Subduction of the Proto-South China Sea (PSCS) beneath NW Sabah began in the Eocene and ceased in the Early Miocene with continent-continent collision between the Dangerous Grounds block (see Figure 1) and the western margin of Sabah. Subsequent continental shortening is responsible for deformation and uplift above sea level of the deep-marine sediments of accretionary complexes such as the Trusmadi and Crocker Formations (Tongkul, 1991, 1994; Hutchison, 2000, 2005; Hall, 2013, 2017). To the northeast, the back-arc extension and opening of the Sulu Sea are frequently associated with SE subduction rollback of the Celebes Sea beneath the Sulu Arc in a time window between ~21 and ~9 Ma (Hall, 2013; Lai et al., 2020).

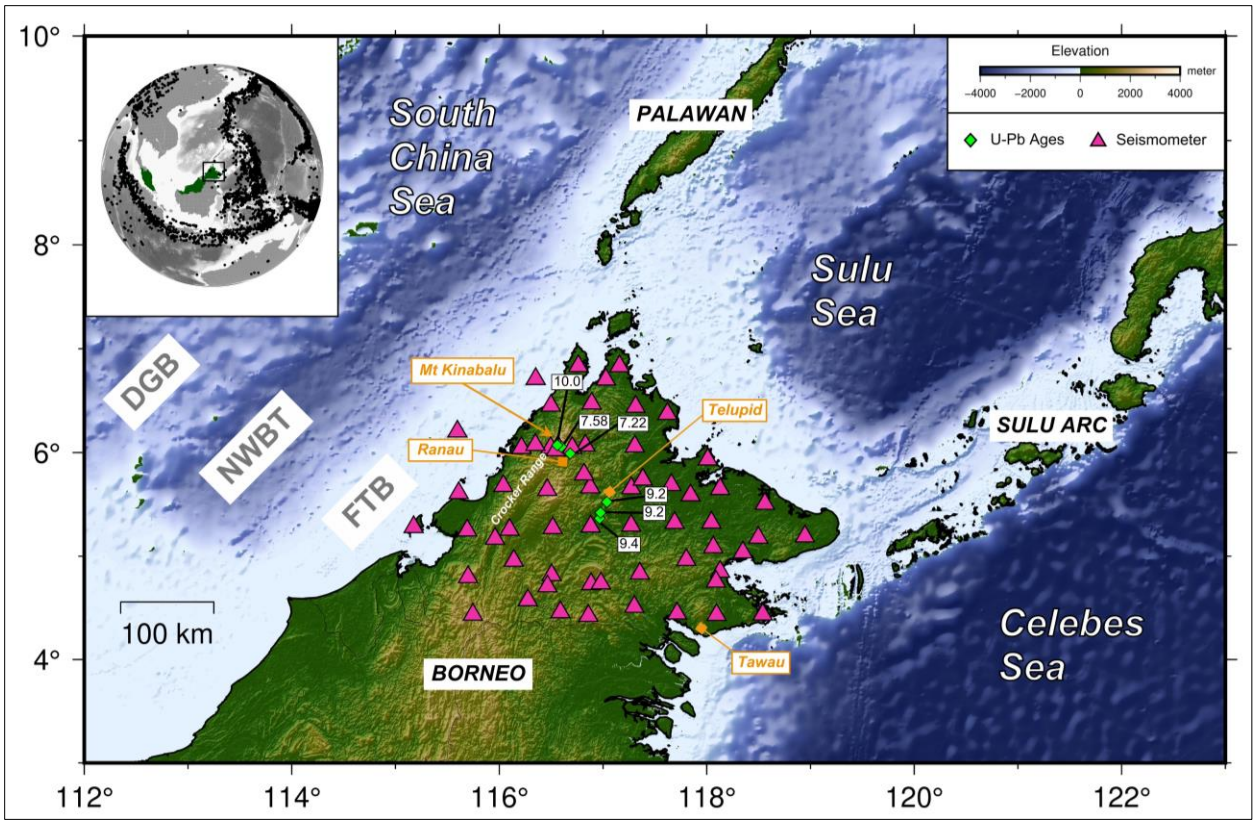

Figure 1. Map of the study area. Magenta triangles show seismic stations from nBOSS and MetMalaysia networks. Green diamonds denote geochemical dating locations relevant to this study. Left inset shows the SE Asia region with Malaysia in green and Sabah highlighted by a black rectangle. DGB, Dangerous Grounds Block; NWBT, NW Borneo Trough; FTB, Fold and Thrust Belt.

A unifying narrative describing the tectonic history of Sabah has proven elusive for various reasons, including the presence of complex geology masked by thick tropical regolith and vegetation, and a lack of information on the crust and underlying mantle structure. From a geochronological perspective, reliable data in the region are limited to only a few clusters (Figure 1); this has prevented previous studies from making robust inferences about significant geological

features and properly constraining the timing of key tectonic developments in Sabah's history. More importantly, the Neogene evolution of northern Borneo and associated neotectonic activity remains controversial, with most explanations lying between two end-member models: (i) compressional tectonics, at least partially associated with the opening of the South China Sea (Tongkul, 1994, 1997; Morley & Back, 2008; Morley et al., 2011) and (ii) extensional tectonics, predominantly driven by trench retreat of the Celebes Sea (Hall, 2013; Pilia et al., 2021a).

Recently, fresh clues have been obtained by Tsikouras et al. (2021) with new zircon radiometric dating of the Ranau peridotites and Telupid ophiolite in Sabah (Figure 1). They suggest that back-arc extension propagated from the Sulu Sea into northern Borneo, resulting in significant extension that led to the exhumation of a subcontinental peridotite suite near Ranau and a rift-related magmatic episode (9.2 to 10.5 Ma) near Telupid. However, this study was subsequently questioned by Cullen and Burton-Johnson (2021), who argue against the interpretation of the new zircon ages by Tsikouras et al. (2021) and the possible extent of propagation of Sulu Sea extension into northern Borneo.

Earthquake data recorded by a new, dense seismic network in Sabah represents an excellent opportunity to constrain many first-order crustal parameters, including thickness and stress orientation. In this study, we estimate Moho depths by exploiting a recently developed passive seismic method commonly referred to as Virtual Deep Seismic Sounding (VDSS), initially proposed by Tseng et al. (2009). We implemented the method as in Thompson et al. (2019) and Pilia et al. (2021b) to get estimates on the crustal thickness beneath the seismic network in northern Borneo. At the same time, we infer the present-day distribution of stress from new focal mechanism analysis of local earthquakes. We then reconcile both sets of results with prior evidence for either a compressional or extensional tectonic setting in northern Borneo.

2 Data Analysis

2.1 Virtual Deep Seismic Sounding

We use waveform data recorded by 46 broadband stations of the northern Borneo Orogeny Seismic Survey (nBOSS) temporary seismic network and 20 broadband stations operated by the Malaysian Meteorological Department (MetMalaysia) (Pilia et al., 2019) – see Figure 1 for locations. We use earthquake events with magnitudes larger than 5.0 in an epicentral distance range between 30° and 50° from the station (Figure 2), resulting in a total of 172 seismic sources. VDSS focuses on the SsPmp phase, originating from an S-to-P conversion under a free surface. The converted P-wave then travels downwards and undergoes a wide-angle (post-critical) reflection at the Moho before impinging on a seismic station (Figure 2). The difference in arrival time between the SsPmp phase and the Ss phase provides an estimate of the Moho depth through the following equation:

$$T_{SsPmp\,-\,Ss} = 2H\,(V_p^{-2} - p^2_{\beta})^{1/2}, \quad (1)$$

where *H* is the crustal thickness, *Vp* is the average P-wave speed in the crust, and p_{β} is the ray parameter, which is determined using the known source-receiver geometry and the ak135 velocity model (Kennett et al., 1995).

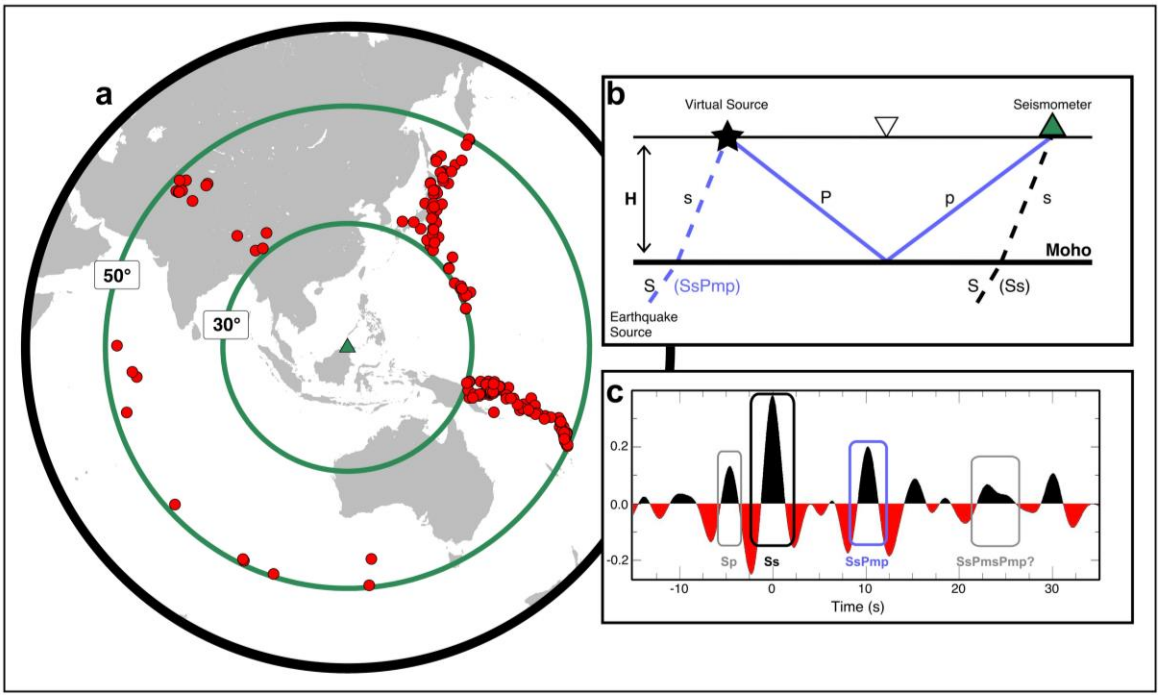

Figure 2. (A) Seismic source distribution (red dots) in the epicentral distance range 30° – 50° from which earthquake data were extracted. (B) The schematic ray diagram illustrates the main phases used during the VDSS analysis. (C) An example of stacked waveform data from a station in Sabah with the Ss and SsPmp arrivals highlighted in black and blue, respectively. The precursor Sp phase and reverberatory SsPmsPmp are also labeled and highlighted in grey.

The first step in preparing a VDSS trace is to isolate the SsPmp phase from its event waveform. This involves windowing data around the S-arrival time generated by a teleseismic source, using predictions from a global reference model (ak135 in this case). The instrument response is then deconvolved from the raw data before applying a second-order zero-phase Butterworth bandpass filter with 0.05 Hz and 0.5 Hz corner frequencies. The horizontal components are subsequently rotated into the radial and tangential components (Thompson et al.,

2019). In order to remove source-side scattering effects, we applied the source normalization method of Yu et al. (2013), which ultimately allows the use of all seismic events within the prescribed epicentral distance range regardless of focal depth. This increases the number of viable waveforms, which is advantageous because the usable epicentral-distance range intrinsic to the method is limited (Figure 2a).

Next, the vertical and radial component traces are rotated into the pseudo-S component traces (Parker et al., 2016; Thompson et al., 2019). These are then deconvolved from the vertical and radial component of the waveform using an extended-time multitaper approach (10 s sliding window, 75% window overlap, 3 Slepian tapers; Helffrich, 2006). The resulting vertical component VDSS traces are then visually inspected and are retained if: (i) the SsPmp phase is clearly visible; ii) a prominent direct Ss arrival and precursor sP can be detected; and iii) ringy or oscillatory signals are absent. Finally, we use the results from a joint receiver function (RF) and surface wave inversion analysis to produce synthetic seismograms to get the predicted travel time of the SsPmp phase for different slowness at each station (Pilia et al., 2021b). Thus, the retained traces (observed data) go through a final inspection where traces are kept if its SsPmp arrival falls within 4-seconds before and after the predicted zero-crossing of the SsPmp in the synthetic seismograms.

At this stage, the only unknown parameter required to estimate the thickness of the crust from Equation (1) is the bulk velocity Vp (Figure S1), which we determined from the joint RF analysis presented in Pilia et al. (2021a). The S-wave velocities estimated beneath each station obtained from the RF analysis are converted to P-wave velocities using the empirical relation devised by Brocher (2005). For each station, we perform a time-to-depth migration of each VDSS trace based on Equation (1) and linearly stack them to produce a final VDSS trace from which the

crustal thickness beneath a station is estimated to be the point where the SsPmp zero-crossing occurs (Pilia et al., 2021b, Tseng et al., 2009, Yu et al., 2016). Due to the post-critical reflection of the P-wave at the Moho, SsPmp undergoes a phase shift, in addition to a clear moveout (Figure S2), that varies across the slowness range between 14.2 and 15.7 sec/deg. The stacking of traces and good slowness coverage of our data averages out any bias that the phase shift might introduce. Calculating the envelope function of the single VDSS traces would remove the phase shift; however, Thompson et al. (2019) show that the zero-crossing proxy and envelope function results are consistent when a good slowness coverage is present, as it is in our case.

The joint RF and surface wave inversion works well in many parts of Sabah but proved challenging, particularly from the perspective of extracting Moho depths, in the east due to the extensive sedimentary basins and the presence of shallow ophiolite cover. The higher frequency content (e.g., 0.05 to 2 Hz) used by RFs appears to be more contaminated by short period noise and reverberations such that the primary phase Ps is not easily identifiable (Figure S3). For VDSS, the primary phase SsPmp recorded in eastern Sabah is more discernible due to the low-frequency content inherent to the method (0.05 to 0.5 Hz), which suppresses undesirable signals arising from small-scale intra-crustal structure beneath Sabah (Figure S4).

2.2 Analysis of Seismicity

We manually picked P-wave first break polarities for 101 earthquakes (Mw $\geq$ 2.0) from a new earthquake catalog for the region around Mt Kinabalu, which were used to calculate moment tensor solutions (Bacon, 2021). This task was performed using the Bayesian moment tensor inversion software MTfit by Pugh (2018), wherein we constrained the solutions to be purely double-couple. MTfit employs a Markov-chain Monte-Carlo approach to explore the posterior

probability space and identify the best-fitting moment tensor solution while naturally incorporating the measurement uncertainties associated with moment tensor estimation (e.g., location and velocity model uncertainties), which can be significant in the case of microseismicity (Figure S5). From the 101 earthquakes analyzed, we produce 26 well-constrained moment tensor solutions (inset in Figure 3; Table S1). These new observations are supplemented by moment tensor solutions recorded in global catalogs (gCMT, ISC-GEM, and GEOFON), reflecting the broader history of seismicity recorded across northern Borneo.

3 Crustal thickness variations in Sabah

Figure 3 illustrates the final Moho-depth map of Sabah obtained using the VDSS method, which reveals several alternating thin and thick crustal bands, with depths ranging between 21 and 46 km. When compared to crustal thicknesses derived from RF analysis (Pilia et al., 2021a) and inferred from the shear wave velocity structure (Greenfield et al., 2022), all three results appear broadly consistent. VDSS has the advantage of obtaining robust depth estimates in the east, where a clear Moho was absent in the RF results (see Figure S6-7). Inferring Moho depth from a shear-wave model constrained by surface waves at best constrains the broadscale pattern of Moho depth, but at least these are largely in agreement with the first-order variations present in the new VDSS model. The robustness of the VDSS results was investigated by constructing Moho maps using the SsPmp bounce points at the Moho as the depth measurement location for different subsets of events (see Figure S8, S9, and S10) and varying the input crustal velocity model by adding random noise

(Figure S11). Overall, our analysis suggests that the features that we interpret are well-constrained by the data.

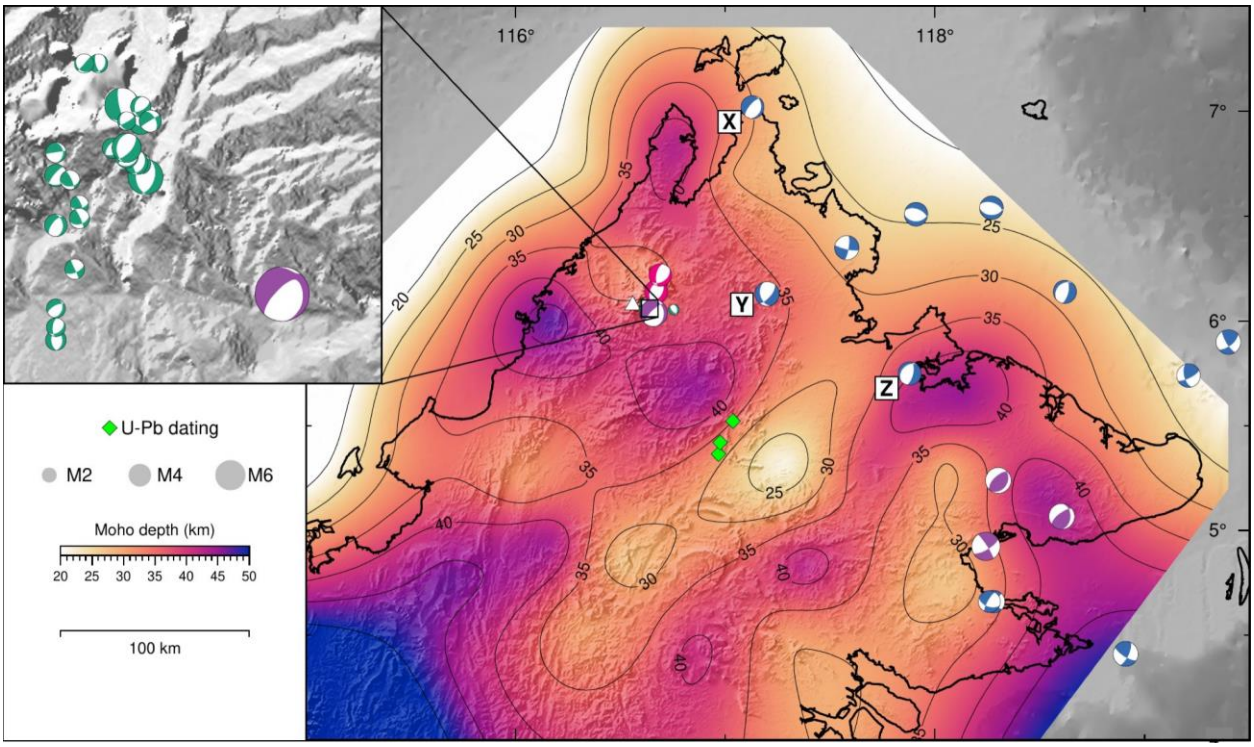

Figure 3. Moho-depth map of Sabah using a color scale centered on 35 km. Green diamonds show the locations of ophiolites of late Miocene age, as inferred by Tsikouras et al. (2021). The white triangle denotes Mt Kinabalu. Black lines are depth-to-Moho contours drawn every 5 km. The top-left inset is a zoom-in of the area around Mt Kinabalu, taken from the area within the square box. Purple focal mechanisms are gCMT solutions, blue are ISC solutions, and red are GEOFON solutions. Green focal mechanisms in the inset map are earthquakes in a new local catalog of seismicity derived from P phase first-motion polarities at stations in the nBOSS and MetMalaysia networks. Focal mechanisms are represented as beachballs plots, scaled by magnitude (scale factor of 2 for inset map).

Following the cessation of PSCS subduction, continent-continent collision occurred in western Sabah, deforming and elevating much of the Crocker Range. The most abrupt deflection of the Moho topography inferred by our results appears to coincide with the Crocker Range, where crustal thickness estimates exceed 40 km in places (Figure 3). This observation suggests that folding and thrusting due to continent-continent collision between western Sabah and the Dangerous Grounds has produced a thicker crust with a substantial root beneath the mountain belt along the western coast. Immediately offshore to the west of the Crocker Range on the continental shelf (thrust and fold belt), the crust is significantly thinner, a result largely compatible with Moho depth inferences made from offshore active seismic methods (Franke et al., 2008).

A significant result that emerges from this study is the area of thin crust that runs from the northeast to the southwest in central Sabah (crust B in Figure 4), with a strike resembling that of the Crocker Range and the NW margin of Sabah. The thin crust is wider at the northeast coast and appears to continue offshore into the Sulu Sea. New radiometric data from Tsikouras et al. (2021) indicate that the chemical signature of the Telupid ophiolite represents that of a narrow oceanic basin. The zircons from the ophiolite are Miocene in age (9.2 to 10 Ma), which is consistent with the timing of back-arc extension induced by slab rollback of the Celebes Sea. Intriguingly, the area of thin crust inferred by our results correlates with the mapped exposure of the Telupid ophiolite and the zircon samples analyzed by Tsikouras et al. (2021). We interpret this area of thin crust as evidence of Miocene extension tectonics likely related to the same back-arc extension that formed the Sulu Sea. Brun et al. (2016) suggest that an acceleration in trench retreat in the Aegean changed the extension mode from localized to distributed. Northern Borneo might have experienced a similar episode during a period of rapid trench rollback of the Celebes Sea ~16 Ma, as suggested

231 by Hall (2013). During this time, extension in the Sulu Sea might have propagated to the SW, thus
232 forming the areas of thin crust we observe in Sabah.

233 In the eastern half of Sabah, the Moho depth map reveals an alternating thick and thin
234 crustal pattern (Figure 3). Despite being narrower than the thick crust labeled A in Figure 4, crust
235 C similarly displays Moho depths of more than 40 km along its strike (see Figure 4). Further
236 southeast, the thin crust that underlies the Tawau area (crust D in Figure 4) could have also resulted
237 from back-arc extension. The overall pattern of an alternating thick and thin crust in Sabah with a
238 common strike is consistent with extensional tectonics where strain localization produces thinner
239 crust between thicker and presumably more resistant blocks, somewhat akin to the style of crustal-
240 scale boudinage observed in the Aegean (Jolivet et al., 2004).

241 The analysis of focal mechanisms observed in Figure 3 provides insight into the present
242 day stress regime in Sabah. A standout feature of the focal mechanism map is that nearly every
243 mechanism is either normal or exhibits a clear extensional component in central and western Sabah
244 (Figure S12). This is not limited to the Ranau area, as indicated by focal mechanisms X, Y, and Z
245 (see Figure 3), adjacent to the thin crustal region in central Sabah revealed by our new Moho depth
246 map. We hypothesize that the western half of Sabah is currently undergoing extension, likely
247 related to orogen collapse, as also suggested by Sapin et al. (2013) based on GPS measurements
248 and study of the NW Borneo Wedge. The orogen collapse may also drive the active fold and thrust
249 belt (FTB) structure observed between the NW Borneo Trough and the Crocker Range (Hall,
250 2013). On the other hand, the east and southeast exhibit more varied focal mechanisms. This could
251 be related to the reorientation of the Celebes Sea tectonic plate, which is now actively subducting
252 southward under Sulawesi.
253

4. Conclusion

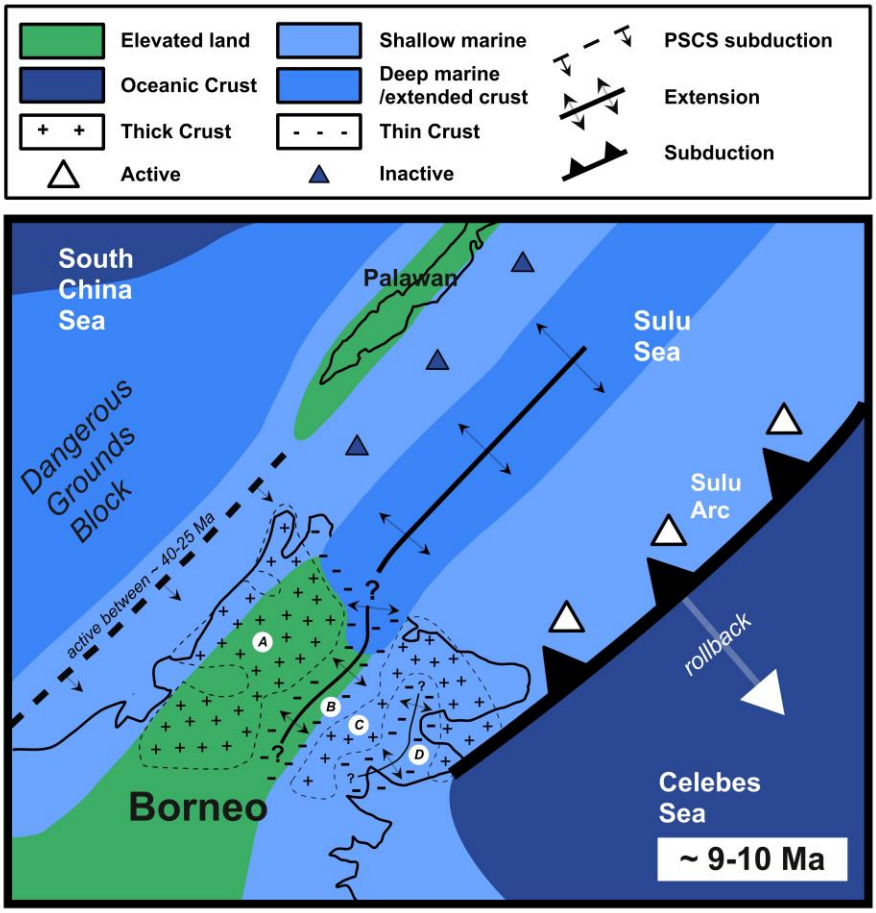

Figure 4. A sketch of the proposed tectonic evolution of northern Borneo (adapted from Hall, 2013; Tsikouras et al., 2021). A and C represent areas of relatively thick crust, while B and D represent areas of relatively thin crust.

Our new crustal thickness model of Sabah, derived from applying the VDSS method to teleseismic waveform data, is consistent with the operation of extensional tectonics throughout much of the Miocene, during which back-arc spreading resulted in the opening of the Sulu Sea. The pattern of trench-parallel thick and thin crust in eastern Sabah is reminiscent of crustal-scale boudinage structures observed elsewhere during subduction rollback and aligns with

interpretations of geochemical and geological data that suggests that Sulu Sea extension propagated into Sabah in the Miocene. Although we cannot rule out the possibility that these crustal thickness variations were present prior to the Sulu Sea opening or were influenced by subsequent events, the confluence of evidence favors extensional rather than compressional tectonics. Our analysis of new and existing focal mechanisms from local earthquakes supports the contemporary stress field being extensional, at least in central and western Sabah, albeit through a different mechanism (orogen collapse) than that invoked for the Miocene. These results show that crustal extension plays an important role in the evolution of post-subduction continental margins, even in the circumstances as complex as northern Borneo, where subduction, continent-continent collision, back-arc extension and orogen collapse have come together to produce a distinctive chain of events.

Acknowledgments

We thank MetMalaysia for allowing access to their restricted data. H.T.L. acknowledges the fieldwork grant awarded by the University of Cambridge through the LWA Research Fund and St Edmunds' Cherry Hume Prize. S.P. acknowledges support from the Natural Environmental Research Council (NERC) Grant NE/R013500/1 and from the European Union's Horizon 2020 research and innovation program under Marie Sklodowska-Curie Grant Agreement 790203. We thank the NERC Geophysical Equipment for loan 1038. Seismic data from the nBOSS network will be accessible through the IRIS Data Management (http://www.iris.edu/mda) from February 2023 (see https://doi.org/10.7914/SN/YC_2018). Waveform data recorded by the northern Borneo Orogeny Seismic Survey network were extracted, quality checked, and archived by C. A. Bacon. Details on the status of this database may be obtained from N.R.

Open Research

The waveform data (VDSS traces) for each station can be downloaded from 10.5281/zenodo.6338668. Data analysis was carried out using C Shell and Python (3.7). The following Python packages were used: ObsPy (1.2.2, Beyreuther et al., 2010) and Numpy (1.21.3, Harris et al., 2020). Data visualization were performed using Generic Mapping Tools (6.0, Wessel et al., 2019) and Matplotlib (3.4.3, Hunter, 2007).

References

Brocher, T. M. (2005). Empirical relations between elastic wavespeeds and density in the earth's crust. *Bulletin of the Seismological Society of America*, 95(6), 2081–2092. https://doi.org/10.1785/0120050077

Bacon, C. A. (2021). Seismic anisotropy and microseismicity: from crustal formation to subduction termination, (Doctoral thesis). Retrieved from Apollo Repository**.** (https://doi.org/10.17863/CAM.82196). Cambridge: University of Cambridge.

Beyreuther, M., Barsch, R., Krischer, L., Megies, T., Behr, Y., & Wassermann, J. (2010). ObsPy: A Python toolbox for seismology. *Seismological Research Letters*, 81(3), 530-533, https://doi.org/10.1785/gssrl.81.3.530

311 Brun, J., Faccenna, C., Gueydan, F., Sokoutis, D., Philippon, M., Kydonakis, K., & Gorini, C.
312 (2016). The two-stage Aegean extension, from localized to distributed, a result of slab
313 rollback acceleration. *Canadian Journal of Earth Sciences*, 53, 1142–1157.
314 https://doi.10.1139/cjes-2015-0203
315
316 Cullen, A., & Burton-Johnson, A. (2021). New zircon radiometric U-Pb ages and Lu-Hf isotopic
317 data from the ultramafic-mafic sequences of Ranau and Telupid (Sabah, eastern Malaysia):
318 Time to reconsider the geological evolution of Southeast Asia?. *Comment: Geology*, 49,
319 e541, https://doi.org/10.1130/G49414C.1
320
321 Franke, D., Barckhausen, U., Heyde, I., Tingay, M., & Ramli, N. (2008). Seismic images of a
322 collision zone offshore NW Sabah/Borneo. *Marine and Petroleum Geology*, 25, 606–624,
323 https://doi:10.1016/j.marpetgeo.2007.11.004
324
325 Greenfield, T., Gilligan, A., Pilia, S., Cornwell, G. D., Tongkul, F., Widiyantoro, S., & Rawlinson,
326 N. (2022). Post-subduction tectonics of Sabah, northern Borneo, inferred from surface
327 wave tomography. *Geophysical Research Journals, Solid Earth*, 49(3),
328 http://doi.org/10.1029/2021GL096117
329
330 Hall, R. (1996). Reconstructing Cenozoic SE Asia, in Hall, R., and Blundell, D., eds., Tectonic
331 Evolution of Southeast Asia. *Geological Society, London, Special Publication 106*, 153–
332 184, https://doi:10.1144/GSL.SP.1996.106.01.11
333

Hall, R., van Hattum, M.W.A., & Spakman, W. (2008). Impact of India-Asia collision on SE Asia. The record in Borneo: *Tectonophysics*, 451, 366–389, https://doi:10.1016/j.tecto.2007.11.058

Hall, R. (2013). Contraction and extension in northern Borneo driven by subduction rollback. *Journal of Asian Earth Sciences*, 76, 399–411, http://doi:10.1016/j.jseaes.2013.04.01

Hall, R., & Spakman, W. (2015). Mantle structure and tectonic history of SE Asia. *Tectonophysics*, https://doi:10.1016/j.tecto.2015.07.003

Hall, R., & Breitfeld, H.T. (2017). Nature and demise of the Proto-South China Sea. *Bulletin of the Geological Society of Malaysia*, 63, 61–76, https://doi:10.7186/bgsm63201703

Harris, C. R., Millman, K. J., van der Walt, S. J., Gommers, R., Virtanen, P., Cournapeau, D., et al. (2020). Array programming with NumPy. *Nature*, 585(7825), 357-362, https://doi.org/10.1038/s41586-020-2649-2

Helffrich, G. (2006). Extended-time multitaper frequency domain cross-correlation receiver-function estimation. *Bulletin of the Seismological Society of America*, 96, 344–347, https://doi:10.1785/0120050098

Hunter, J. D (2007). Matplotlib: A 2D graphics environment. *Computing in Science & Engineering*, 9(3), 90-95, https://doi.org/10.1109/MCSE.2007.55

Hutchison, C.S. (2005). Geology of north-west Borneo. *Elsevier*, 351-356, https://doi.org/10.1016/B978-0444519986/50028-4

Hutchison, C.S., Bergman, S.C., Swauger, D.A., & Graves, J.E. (2000). A Miocene collisional belt in north Borneo. Uplift mechanism and isostatic adjustment quantified by thermochronology. *Journal of the Geological Society*, 157, 783–793, https://doi:10.1144/jgs.157.4.783

Jolivet, L., Famin, V., Mehl, C., Parra, T., Aubourg, C., Hebert, R., & Philippot, P. (2004). Strain localization during crustal-scale boudinage to form extensional metamorphic domes in the Aegean Sea. *Geological Society of London Special Publication*, 380, 185–210, https://doi.org/10.1130/0-8137-2380-9.185

Kennett, B.L.N., Engdahl, E.R., & Buland, R. (1995). Constraints on seismic velocities in the Earth from traveltimes. *Geophysical Journal International*, 122, 108–124, https://doi:10.1111/j.1365-246X.1995.tb03540.x

Lai, C.K., Xia, X.P., Hall, R., Meffre, S., Tsikouras, B., Rosana Balangue-Tarriela, M.I., Idrus, A., Ifandi, E., & Norazme, N. (2021). Cenozoic evolution of the Sulu Sea Arc-basin system. An overview. *Tectonics*, 40, 1–26, https://doi:10.1029/2020TC006630

Morley, C.K., & Back, S. (2008). Estimating hinterland exhumation from late orogenic basin volume, NW Borneo. *Journal of the Geological Society*, 165, 353–366, https://doi.org/10.1144/0016-76492007-067

Morley, C.K., King, R., Hillis, R., Tingay, M., & Backe, G. (2011). Deepwater fold and thrust belt classification, tectonics, structure and hydrocarbon prospectivity. A review: *Earth-Science Reviews*, 104, 41–91, https://doi:10.1016/j.earscirev.2010.09.010

Parker, E. H., Hawman, R. B., Fischer, K. M. & Wagner, L.S. (2016). Estimating crustal thickness using SsPmp in regions covered by low-velocity sediments: imaging the Moho beneath the Southeastern Suture of the Appalachian Margin Experiment (SESAME) array, SE Atlantic Coastal Plain. *Geophysical Research Letters*. 43(18), 9627-9635, https://doi.org/10.1002/2016GL070103

Pilia, S., Davies, D.R., Hall, R., Bacon, C., Gilligan, A., Greenfield, et. al. (2021a). Effects of post-subduction processes on continental lithosphere. https://doi.org/10.21203/rs.3.rs-861968/v1

Pilia, S., Rawlinson, N., Gilligan, A., & Tongkul, F. (2019). Deciphering the fate of plunging tectonic plates in Borneo. Eos, *Transactions American Geophysical Union 100*, 18-23, https://doi.org/10.1029/2019EO123475

Pilia, S., Ali, M.Y., Searle, M.P., Watts, A.B., Lü, C., & Thompson, D.A. (2021b). Crustal structure of the UAE-Oman mountain range and Arabian rifted passive margin: New constraints from active and passive seismic methods. *Journal of Geophysical Research, Solid Earth*, 126, https://doi:10.1029/2020JB021374

Pugh, D.J., & White, R. S. (2018). MTfit: A Bayesian Approach to Moment Tensor Inversion**.** *Seismological Research Letters*, 89, 1507–1513, https://doi.org/10.1785/0220170273

Rangin, C., Jolivet, L., & Pubellier, M. (1990). A simple model for the tectonic evolution of Southeast Asia and Indonesia region for the past 43 m.y. *Bulletin de la Société Géologique de France*, 6, 889–905, https://doi.org/10.2113/gssgfbull.VI.6.889

Sapin, F., Hermawan, I., Pubellier, M., Vigny, C., & Ringenbach, J-C. (2013). The recent convergence on the NW Borneo Wedge. A crustal-scale gravity gliding evidenced from GPS. *Geophysical Journal International*, 193, 549-556, https://doi:10.1093/gji/ggt054

Thompson, D.A., Rawlinson, N., & Tkalčić, H. (2019). Testing the limits of virtual deep seismic sounding via new crustal thickness estimates of the Australian continent. *Geophysical Journal International*, 218, 797–800, https://doi:10.1093/gji/ggz191

Tongkul, F. (1991). Tectonic evolution of Sabah, Malaysia. *Journal of Southeast Asian Earth Sciences*, 6, 395–405, https://doi:10.1016/0743-9547(91)90084-B

Tongkul, F. (1994). The geology of Northern Sabah, Malaysia: Its relationship to the opening of the South China Sea Basin. *Tectonophysics*, 235, 131–147, https://doi:10.1016/0040-1951(94)90021-3

Tongkul, F. (1997). Polyphase deformation in the Telupid area, Sabah, Malaysia. *Journal of Asian Earth Sciences*, 15, 175–183, https://doi.org/10.1016/S0743-9547(97)00006-8

Tseng, T.L., Chen, W.P., & Nowack, R.L. (2009). Northward thinning of Tibetan crust revealed by virtual seismic profiles. *Geophysical Research Letters*, 36, 1–5, https://doi:10.1029/2009GL040457

Tsikouras, B., La, C.K., Ifandi, E., Norazme, N.A., Teo, C.H., & Xia, X.P. (2021). New zircon radiometric U-Pb Ages and Lu-Hf isotopic data from the ultramafic-mafic sequences of Ranau and Telupid (Sabah, East Malaysia): Time to reconsider the geological evolution of Southeast Asia? *Geology*, 49, 789–793, https://doi:10.1130/G48126.1

Wessel, P., Luis, J., Uieda, L., Scharroo, R., Wobbe, F., Smith, W., & Tian, D. (2019). The Generic Mapping Tools version 6. *Geochemistry, Geophysics, Geosystems,* 20(11), 5556-5564, https://doi.org/10.1029/2019GC008515

Yu, C.Q., Chen, W.P., & van der Hilst, R.D. (2013). Removing source-side scattering for virtual deep seismic sounding (VDSS). *Geophysical Journal International*, 195, 1932–1941, https://doi:10.1093/gji/ggt359